

Double-pass spectroimaging with spectral multiplexing: TUNIS

A. López Ariste, C. Le Men and B. Gelly

THEMIS. CNRS UPS 853. Spain

(E-mail: arturo@themis.iac.es)

Received: December 31, 2010; Accepted: July 12, 2011

Abstract. Solar observations would benefit from simultaneous imaging and spectroscopy. To approach in an optimal manner such an ideal goal we have designed and built in THEMIS a spectro-imager based upon the concept of subtractive double pass through a diffraction grating spectrograph called TUNIS. In its basic design it produces an image at a wavelength which changes linearly in one of the directions of the image. To improve the simultaneity of the spectral coverage, we have implemented a spectral multiplexing, based upon Hadamard spectroscopy. We present the first observations of TUNIS and give the main specifications. TUNIS has been proposed for the European Solar Telescope (EST) project.

Key words: Techniques: imaging spectroscopy

1. Introduction

The observation of the solar atmosphere is rapidly requiring to break technological barriers. It is not enough to take a picture at a given wavelength ignoring what happens at neighboring wavelengths, ignoring that, for example, brightenings may just be Doppler shifts of a line. Nor is it acceptable to observe the spectrum of a point without the possibility to put it in the context of what neighboring points are doing at the same instant of time: has a feature just disappeared or has it merely been advected beyond the slit?

Observing full images with full spectra as simultaneously as possible and at the fastest cadence affordable: that has to be the goal of any new instrument for present solar telescopes, but even more crucial for future telescopes like the European Solar Telescope (EST).

Tunable Universal Narrowband Imaging Spectrograph (TUNIS) is a recently commissioned instrument that addresses solar observations with that goal in mind. It has been built in THEMIS and is also proposed for EST. TUNIS is a spectroimager, based upon the concept of subtractive double-pass. To recover the full spectra, TUNIS implements a multiplexing scheme using Hadamard spectral techniques. Both concepts, subtractive double-pass spectroimaging and multiplexing with Hadamard techniques, are explained in the next two sections. First results and some comments on image quality and noise concerns are left for the last section.

2. Imaging through spectrograph: subtractive double pass

Let us simplify a spectrograph into a linear mapping of the light intensity distribution $f(x, y; \lambda)$ at the entrance focal plane of the instrument onto $F(X, Y)$ at the exit focal plane. We neglect non-linearities in the dispersion of wavelength or geometrical aberrations introduced by the spectrograph optics without any loss of generality. The dispersion element (an echelle grating for example) will send light of a particular wavelength into a discrete set of angular directions that we refer to as orders. Let us suppose, in the same spirit just exposed, that all the light of the spectral domain observed concentrates in a given single order. The illuminated order presents a linear dispersion D (in Å/mm for example) at the output focal plane and we can write that

$$F(X, Y) = \int_{\lambda_0}^{\lambda_1} \delta\left(\alpha x + \frac{\lambda}{D} - X\right) \delta(\beta y - Y) f(\alpha x, \beta y; \lambda) d\lambda, \quad (1)$$

where λ_0 and λ_1 give the limits of the observed spectral domain, and α and β would represent optical zooms introduced by the spectrograph optics. For simplicity, we shall assume them to be unity from this point on.

The previous basic relationship expresses the fundamental fact that in the direction of dispersion, here chosen to be on the X axis, there is a mixing of information (of light intensity) coming from all points x in the entrance focal plane at those wavelengths λ that fulfill the relationship $X = x + \lambda/D$. A traditional spectrograph solves such mixing of spatial and spectral information by limiting the field of view at the entrance focal plane with a *slit* at x_0 that we can represent as:

$$f(x, y; \lambda) \equiv \delta(x - x_0) f(x, y; \lambda). \quad (2)$$

With it, the mapping at the exit focal plane an intensity map changes as follows:

$$F(X, Y) = \int_{\lambda_0}^{\lambda_1} \delta\left(x_0 + \frac{\lambda}{D} - X\right) \delta(y - Y) f(x_0, y; \lambda) d\lambda = D f(x_0, Y; D(X - x_0)). \quad (3)$$

That is, in the direction of dispersion the only information left corresponds to a unique image point (x_0, y) at varying wavelengths for varying X . In such a way a simple measurement of the light intensity F at different positions X allows a measurement of the spectral distribution of the image point at x_0 .

But to do imaging we cannot use a narrow entrance slit. It should be opened and we recover at the output plane the mixture of light coming from different points of the field at different wavelengths. But rather than measuring directly the light at that plane, we place there a *spectral slit* $\delta(X - X_0)$. Such slit will let pass each and every point of the image, following the expression above, but only at a single wavelength λ , the one that, given the coordinate x on the image, satisfies the relationship

$$x + \frac{\lambda}{D} = X_0. \quad (4)$$

Notice that different points x of the image can now be differentiated by their different wavelengths. And this is the purpose of the second pass through the spectrograph: to reform the image by sending the light from different points x to different angles using the fact that they have been transmitted at a unique wavelength λ .

If the spectral slit is not infinitely narrow but has a finite width, that width will constrain and define the spectral resolution of the instrument. Thus spectral and spatial resolutions are not coupled, unlike in traditional spectrographs where modifying slit width immediately translates into a change in spatial and spectral resolutions. But also notice that for finite widths, there is still a distribution of wavelengths going through the spectral slit. The second pass will in consequence do more than just sending different points of the original image to different points of the output image. It will also spread, for each point, all the wavelengths that go through the slit. Admittedly, this may be a small effect (at the high spectral resolutions required for solar observations this width is the equivalent of just 20 or 30 mÅ). But it can be easily larger than the spatial resolution of our instrument and there will be a spectral smearing of each point. To avoid this smearing of the output image the second pass through the spectrograph is made as to match the dispersion of the first pass but in the opposite sense. Thus the original dispersion of the wavelengths that pass through the spectral slit will just be subtracted and the smearing will disappear. This is the basic explanation of a spectroimager based upon subtractive double-pass as TUNIS, and its predecessors (Mein, 1977, 1989, 1991, 2001; Stenflo, 1973; Berlicky *et al.*, 2006; López Ariste *et al.*, 2010).

3. Multiplexing with Hadamard masks

A single spectral slit maps each point of the image in the entrance plane of the instrument onto a single point at the output image at a unique wavelength. If for each point we want to recover full spectra, it can be proposed to scan the spectra over the image. Such scan is feasible but it does not help in our goal to achieve simultaneous image and spectrum. Because of this reason TUNIS goes beyond the single spectral slit concept introduced in the previous section.

Let us open a second slit at X_1 in the model of the previous section. At the output plane of the second pass, the image point (x, y) has been mapped onto coordinates (w, z) for wavelength λ_{X_0} and also for wavelength λ_{X_1} . The image at that output plane is still right since there has only been a shift in wavelengths of the image passing through the slit X_1 with respect to the image passing through the slit X_0 . Thus at every point at the output image we are measuring two wavelengths simultaneously. To recover the intensities at each one

of the two wavelengths we need a second measurement. For example, one could imagine that for the second measurement one of the slits is closed so that we only measure the intensity of the other wavelength. In this trivial multiplexing scheme one wavelength is measured in only one of the exposures while the other is measured in both of them. We argue that this is an improvement in terms of approaching simultaneity with respect to a scheme in which each wavelength would be measured independently. Obviously, in the case of two slits we have chosen for illustration the improvement is not worth the effort. But we can carry on with the idea and ask whether there are patterns of opened and closed slits that balance the exposure times and signals for all involved wavelengths so that we can argue that all of them are measured almost simultaneously even if it is during a sequence of exposures. Multiplexing schemes as the one we are seeking are abundant in the scientific literature. We found useful to use Hadamard matrices (Nelson & Fredman, 1970). Multiplexing with them has one big advantage: the matrices are cyclical, and changing from one set of opened slits to the next one is made with a simple mechanical shift of a double mask under an absolute mask.

Hadamard matrices are known for many dimensions, that is, for many different number of simultaneously measured wavelengths. We have chosen one of dimension 31. Actually, Hadamard matrices are made of $+1$ and -1 entries that would require us to observe both the light that goes through the opened slits and the light that goes through the closed ones. The implementation of this in TUNIS proved to be unfeasible so we used a pseudo-Hadamard matrix made of $+1$ and 0 's. The physical mask was photo-deposited on a glass plate and placed under a fixed mask. This *Hadamard mask* can be seen in Fig. 1. Measuring through such a mask produces an image in which each point is made of the addition of 17 different wavelengths out of the 31 wavelengths multiplexed. 31 such measures are made with different 17 slits opened cyclically. Examples of those images can be seen in Fig. 2. The 31 images are then multiplied by the inverse Hadamard matrix to retrieve the spectra (31 wavelengths) for each point in the image.

4. Specifications of TUNIS, image quality and noise issues

TUNIS has been built using the THEMIS echelle spectrograph, with a focal length for both the collimator and camera mirrors of roughly 8 m. The typical dispersion at the useful orders is of $5 \text{ mm}/\text{\AA}$. Combined with the scale plate of the image, we find a characteristic figure of $14.5 \text{ arcsec}/\text{\AA}$. That number gives the relationship between the spatial scale and the dispersion along the direction of the image shared by both scales. The total field of view can be as large as $2 \times 2 \text{ arcmin}$ but it is often smaller to allow for smaller pixels ($0.2 \text{ arcsec}/\text{pixel}$ sampling at most). At all possible configurations the pixels are bigger than the diffraction limit of the telescope which results in some aliasing and into a hard

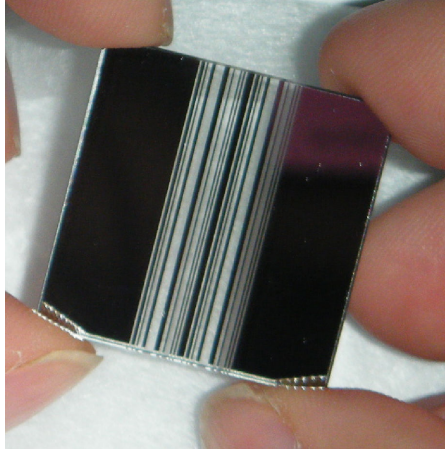


Figure 1. Hadamard mask. 31 slits (17 open) repeated twice. Spectral width of $30 \text{ m}\text{\AA}$.

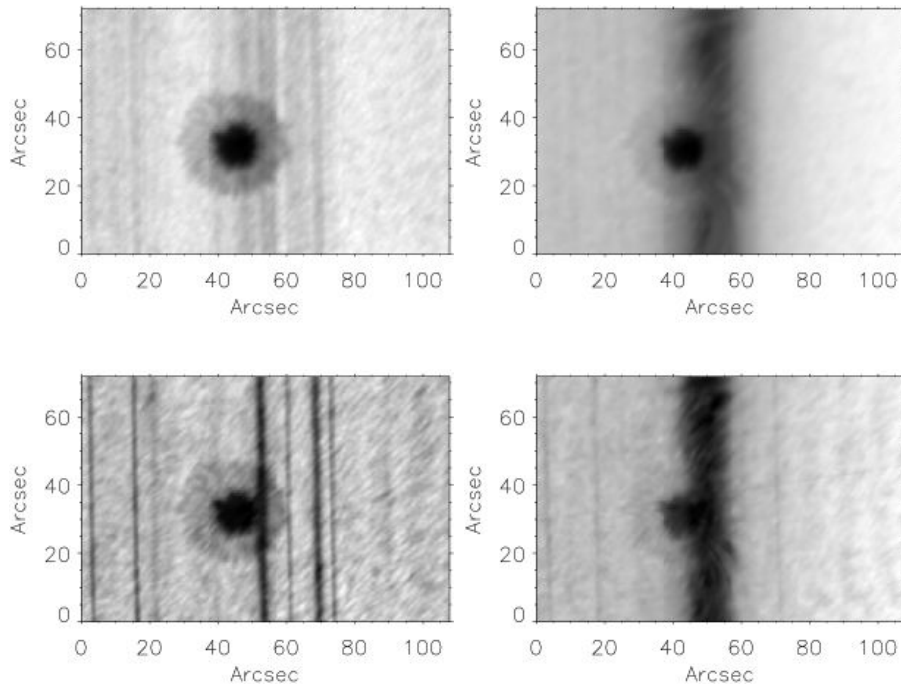


Figure 2. Observing with TUNIS in Fe 630 nm (left) and $H\alpha$ (right) with a spectral resolution of $30 \text{ m}\text{\AA}$ and 10 ms of exposure time. Above the multiplexed raw images, below the demultiplexed ones.

lower limit to spatial resolution. Transmission has been estimated, near the blaze angle of the diffraction grating, at 40%, including the sensitivity of the detector.

The Hadamard mask installed in TUNIS is of dimension 31, with a bandwidth of 30 mÅ. At any exposure along the Hadamard cycle, 17 slits out of 31 are open. In wavelengths near the blaze angle the sum of those 17 intensities saturates the pixels of the camera ($150000 e^-$) in 1 to 2 ms. Such short exposures open the door to image post-reconstruction techniques and a fast polarimetric modulation.

Image quality with TUNIS has been measured with a home-made curvature wave-front sensor observing a pinhole at the entrance of the instrument. Typical rms amplitudes of the measured wavefront are of $\lambda/10$ and are mostly dominated by spectrograph seeing. Thus the instrument can potentially reach the diffraction limit of the telescope. This measurement is often misunderstood because of the belief that diffraction gratings are not good for imaging. This belief is often apparently supported by the surface quality figures given by grating constructors which are typically of the order of $\lambda/2$. To understand those two figures of merit of the wavefront, and their impact in image quality, we consider the three different surfaces of interest in a diffraction grating. The smallest one is the mirror face of the grooves. Their size is such that any deformation of their specular surface introduces aberrations of order bigger than 1000 in terms of Zernike polynomials. Such deformations result in scattered light but not in image degradation. Next we consider the disposition of grooves one respect to the others. Any misalignment of this kind would result in ghosts and other spectral issues that are also sometimes observed but which are absent or almost negligible in scientifically used instruments. The third class is the global shape of the grating which may not be flat. This is what the $\lambda/2$ value usually refers to: the global shape of the grating is a flat plane up to that level of precision. The most common departure from flatness is of course defocusing, followed by astigmatism and coma. Defocusing is automatically corrected during the tuning of the instrument. Our curvature wavefront sensor did not detect any residual astigmatism or coma at the specified limit.

A final concern is noise. If the full Hadamard matrix was used one would expect to retrieve equal noise amplitudes with and without multiplexing. Actually if our detectors were dominated by readout (additive) noise, a smaller noise (the Fellgett advantage) in the data is expected through the use of the Hadamard multiplexing. TUNIS detectors are dominated by photon (multiplicative) noise and such advantage disappears. Furthermore, the use in TUNIS of the modified Hadamard matrices with closed slits further translates roughly into a $\sqrt{2}$ penalty in noise because of the light lost in the close slits.

An extra source of noise appears when wavelengths with very low intensities (at the core of spectral lines for example) are multiplexed with wavelengths in the continuum. In the case of photon noise, the total noise is given by the square root of the total number of photons, dominated by the intensity in the continuum. Thus, the wavelengths at the core of a spectral line carry a noise not

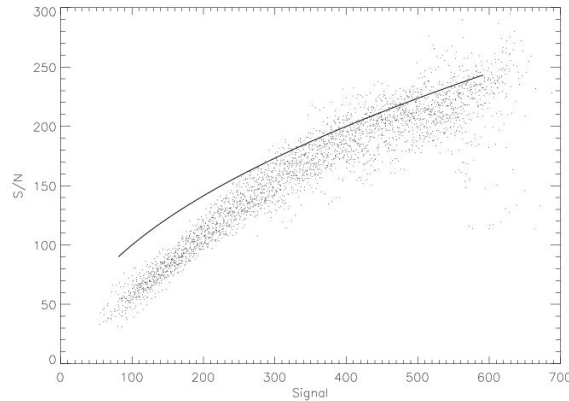


Figure 3. Noise penalty for low intensities multiplexed with high intensities. The thick line shows the square root law for comparison.

proportional to the square root of their intensity, but to the square root of the intensity of the continuum, a much bigger value. This is a second noise penalty implicit to the Hadamard multiplexing. A measure of this effect in TUNIS data is shown in Fig. 3.

Acknowledgements. Many thanks are due to J. Koza, who thoroughly read through this manuscript and, among several other comments, correctly integrated equation (3) to make it appear as shown.

References

- Berlicki, A., Mein, P., Schmieder, B.: 2006, *Astron. Astrophys.* **445**, 1127
 López Ariste, A., Le Men, C., Gelly, B., Asensio Ramos, A.: 2010, *Astron. Nachr.* **331**, 658
 Mein, P.: 1977, *Sol. Phys.* **54**, 45
 Mein, P.: 1989, in *Proceedings of the 10th Sacramento Peak Summer Workshop: High spatial resolution solar observations*, ed.: Oskar von der Lühe, National Solar Observatory, Sunspot, New Mexico, 195
 Mein, P.: 1991, *Astron. Astrophys.* **248**, 669
 Mein, P.: 2002, *Astron. Astrophys.* **381**, 271
 Nelson, E.D., Fredman, M.L.: 1970, *Journal of the Optical Society of America* **60**, 1664
 Stenflo, J.O.: 1973, *Applied Optics* **12**, 805